APPLICATION OF SIMILARITY MAPPING IN DYNAMIC POSITRON EMISSION TOMOGRAPHY STUDIES

T. Thireou[1], G. Kontaxakis[2], A. Dimitrakopoulou-Strauss[3], L. Strauss[3], S. Pavlopoulos[1], A. Santos[2]

[1] Biomedical Engineering Laboratory, National Technical University of Athens, Greece
[2] E.T.S.I. de Telecomunicación, Universidad Politécnica de Madrid, Spain
[3] Medical PET Group-Biological Imaging, German Cancer Research Center, Heidelberg, Germany

Abstract

Dynamic ^{18}F-fluorodeoxyglucose positron emission tomography (PET) studies can successfully be used for diagnosis, therapy planning and monitoring in oncology. Using similarity mapping, we assessed the accuracy of anatomical localization of lesions and the detectability of metastases. 17 patients with colorectal cancer and 3 patients with plasmocytoma were included in the study. All dynamic ^{18}F-FDG PET data sets were iteratively reconstructed and the 55-60 min SUV (standardized uptake values) were estimated. Similarity maps were calculated using reference tumor volumes of interest according to four similarity measures (correlation coefficient, normalized correlation coefficient, sum of squares normalized correlation coefficient, squared sum normalized correlation coefficient). The latter provided the best similarity maps in all cases delineating malignant lesions and enhancing the detectability of metastases. We show that similarity mapping has a significant clinical value in identifying image structures in dynamic PET studies.

1. Introduction

Positron emission tomography provides physicians with unique diagnostic information which may improve patient management and reduce the total cost of patient care. It produces images of molecular-level physiological function, which can be used to measure many vital processes, such as glucose metabolism, blood flow and oxygen utilization.

PET permits the assessment of chemical and physiological changes related to metabolism. This is important because functional change often predates structural changes in tissues. PET images may therefore demonstrate pathological changes long before they would be revealed by modalities like computerized tomography (CT) and magnetic resonance imaging (MRI). Unlike traditional nuclear medicine, PET uses unique radiopharmaceuticals that are the basic elements of biological substrates. These isotopes mimic natural substrates such as sugars, water, proteins, and oxygen. As a result, PET will often reveal more about the cellular-level metabolic status of a disease than other types of imaging modalities.

After extensive investigation in experimental and clinical oncology, ^{18}F-fluorodeoxyglucose (^{18}F-FDG) PET has been proved to be a valuable imaging technique for the evaluation of a variety of tumors. Dynamic ^{18}F-FDG PET studies (temporal sequences of images at the same bed position) offer differential diagnostic information and has increasingly been used for diagnosis, therapy management and evaluation. Several methods have been proposed for the analysis of such studies, in order to increase the accuracy of localizing primary tumors and metastases and to improve the prognosis of patients [1,2]. In this context, we have investigated the performance of similarity mapping (SM).

In SM, the similarity between the time activity curve (TAC) of each pixel and the TAC of a reference region of interest (ROI) is calculated and displayed as an image (similarity map). The similarity map segments the image into regions according to their temporal rather than spatial properties [3]. SM images therefore provide spatially differentiated quantitative information describing the physiological behavior of the images structure, which often can not be extracted from the visual inspection of dynamic PET image sequences. Several measures can describe the similarity [4]: covariance function, cross-correlation, difference, Tanimoto similarity coefficient.

In this work we present the application of the similarity mapping method in dynamic PET images of cancer patients.

2. Materials and Methods

The study included 17 patients with colorectal tumor recurrences and 3 patients with plasmocytoma. The final diagnosis was confirmed by histopathology. After intravenous injection of 300-370 MBq ^{18}F-FDG, 23 frames were acquired for 60 min (10 frames of 1 min, 5 frames of 2 min, and 8 frames of 5 min) using an ECAT EXACT HR+ tomograph [5,6]. After scatter and attenuation correction, the data were iteratively reconstructed [7] (weighted least-square method, ordered subsets, four subsets, six iterations, image matrix: 128×128 pixels) and the 55-60 min SUV [8] were calculated.

Four similarity measures were used for the calculation of similarity maps: Correlation coefficient *COR*, normalized correlation coefficient *NCOR*, sum of squares normalized correlation *SSQNCOR,* and squared sum normalized correlation *SQSNCOR*:

$$COR_{ij} = \frac{\sum_{n=1}^{N} A_{ijn} R_n}{\sqrt{\sum_{n=1}^{N} A_{ijn}^2 \sum_{n=1}^{N} R_n^2}} \quad (1)$$

$$NCOR_{ij} = \frac{\sum_{n=1}^{N} (A_{ijn} - \mu_{Aij})(R_n - \mu_R)}{\sqrt{\sum_{n=1}^{N} (A_{ijn} - \mu_{Aij})^2 \sum_{n=1}^{N} (R_n - \mu_R)^2}} \quad (2)$$

$$SSQNCOR_{ij} = \frac{\sum_{n=1}^{N} (A_{ijn} - \mu_{Aij})^2 (R_n - \mu_R)^2}{\sqrt{\sum_{n=1}^{N} (A_{ijn} - \mu_{Aij})^2 \sum_{n=1}^{N} (R_n - \mu_R)^2}} \quad (3)$$

$$SQSNCOR_{ij} = \frac{(\sum_{n=1}^{N} (A_{ijn} - \mu_{Aij})(R_n - \mu_R))^2}{\sqrt{\sum_{n=1}^{N} (A_{ijn} - \mu_{Aij})^2 \sum_{n=1}^{N} (R_n - \mu_R)^2}} \quad (4)$$

where N is the number of frames, M is the number of slices, A_{ijn} is the value of pixel (i, j) in frame n, R_n is the value of the reference ROI TAC, μ_R is the mean value of the reference TAC and μ_{Aij} is the mean value of the pixel (i, j) TAC. A reference volume of interest (VOI) over the tumor instead of a reference ROI was used, in order to improve the statistical properties of the TAC.

Both correlation and normalized correlation maps have values ranging from –1 (for regions that are perfect "negatives" of R_n) to +1 (for regions which are identical to the reference TAC). While both measures are normalized for proportional differences, only the *NCOR* is normalized for additive differences [3]. *SSQNCOR* and *SQSNCOR* provide a similarity measure normalized for additive differences and perfect negatives and have values ranging from 0 (for totally uncorrelated regions) to a maximum value different in each case.

3. Results

The time required for the analysis of a complete data set (23 frames, 32 slices per frame, 128×128 pixels per slice) was 40 sec for the calculation of the SM. Figure 1 shows an example of four similarity maps calculated according to equations (1)-(4) for the same transaxial image slice of one data set. In all 20 patient studies, similarity maps based on the correlation coefficient and the normalized correlation coefficient were very noisy and the tumors could not be separated from the other structures.

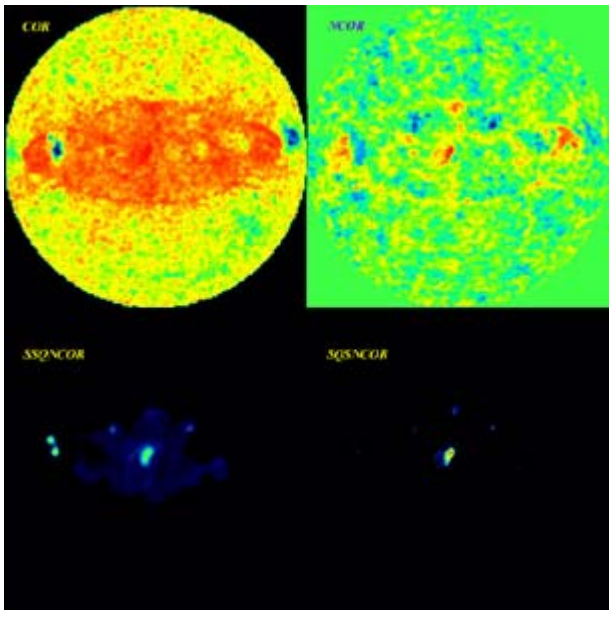

Figure 1: Similarity Maps of the same image slice calculated using the tumor VOI according to the *COR* (upper left), *NCOR* (upper right), *SSQNCOR* (lower left) and *SQSNCOR* (lower right) formulas

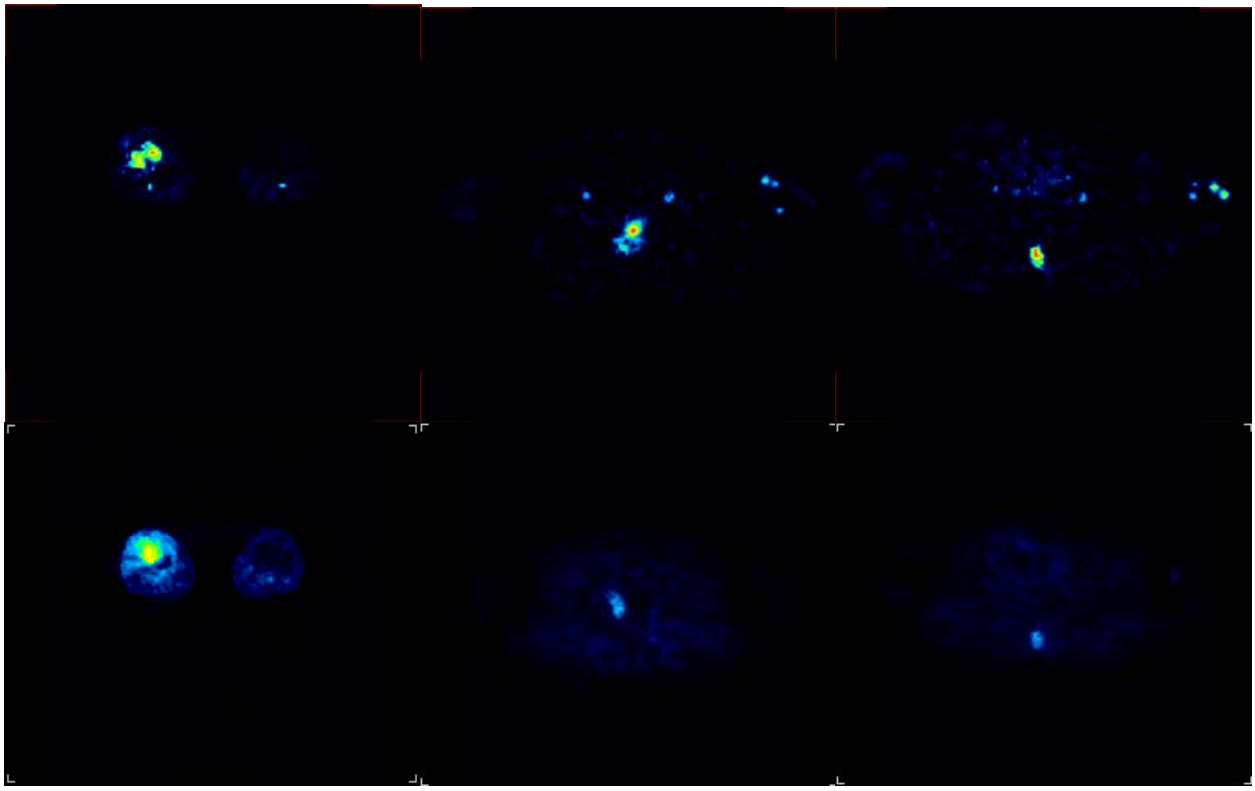

Figure 2. Similarity maps (upper row) and SUV images (lower row) from three transaxial slices from dynamic PET studies of patients with a plasmocytoma of the right tibia (left column) and recurrent colorectal tumor (middle and right columns)

In the sum of squares normalized correlation coefficient similarity map, both the tumor and the vessels were present, whereas in the squared sum normalized correlation coefficient similarity map the tumor was the only predominant structure. Since both measures are normalized for "negative" differences, regions with almost opposite time activity curves such as the tumor and the vessels have similar values and are visible in the resulting map. However, the *SQSNCOR* enhance the differences and provides better results in revealing the structures of interest.

Figure 2 shows a comparison of SM images (*SQSNCOR,* upper row) vs. SUV images of the same studies (lower row). The left column shows a transaxial slice from a dynamic PET study of a patient with a plasmocytoma of the right tibia. SUV images show an enhanced FDG uptake in the center of the lesion, while the peripheral parts of the tumor show a more diffused enhanced FDG uptake. The SM image demonstrates two parts of the giant cell tumor with enhanced FDG uptake with a different distribution pattern than conventional SUV image. Furthermore, the vessels are well delineated. The middle and right columns show two transaxial slices from dynamic PET studies of two patients with recurrent colorectal tumor. The lesions are well delineated in the SUV image (presacral). In the SM image the tumors show better contrast than in the SUV images and the vessels are clearly delineated.

Prior to the calculation of similarity maps, the dynamic images should be checked for proper spatial registration [3]. Another consideration is the need of manual selection of the reference VOI by an operator according to the clinical question being asked. This procedure can be time consuming, subjective and prone to operator bias. Research is ongoing for the development of a semi-automatic technique for the optimum selection of reference ROI by testing many possible reference pixels using a maximum entropy method [11].

4. Conclusions

Although similarity mapping has successfully identified various structures in dynamic MRI data sets

[3, 4, 9, 10], it has not yet been applied to dynamic PET data sets.

Our study showed that the *SQSNCOR* similarity map rapidly identifies structures with similar to the tumor temporal properties and enhances the detection of metastases that are not easily discriminated in the SUV images due to poor image quality or lesions characteristics (size, location etc). Therefore, similarity mapping based on the squared-sum normalized correlation coefficient measure could successfully be used in the analysis of dynamic ^{18}F-FDG PET data sets in oncology to support the visual interpretation of the studies.

Acknowledgements

This work has been partly supported by a scientific cooperation project between Spain and Greece, sponsored by the Spanish Ministry of Foreign Affairs and the Greek Ministry of Development, project TIC2001-0175-C03 from Spanish Government and III PRICIT from Comunidad de Madrid. T. Thireou acknowledges support by the State Fellowships Foundation (IKY, 32nd Fellowships Programme for Graduate Studies) of Greece for doctoral studies in the field of Biomedical Technology.

Address for correspondence:

George Kontaxakis, PhD
Dpto. de Ingeniería Electrónica
E.T.S.I. de Telecomunicación
Universidad Politécnica de Madrid
Ciudad Universitaria s/n
28040 Madrid, Spain

e-mail: gkont@die.upm.es
web: http://www.die.upm.es/im/

References

[1] L.G. Strauss, G. Kontaxakis, A. Dimitrakopoulou-Strauss, S. Pavlopoulos, A. Santos Lleo. Parametric imaging of dynamic PET studies, based on compartmental and non-compartmental approaches. *Europ. J. Nucl. Med*., 25(8): 938, 1998

[2] T. Thireou, L. Strauss, G. Kontaxakis, S. Pavlopoulos, A. Santos. Principal Component Analysis in Dynamic PET, *Conf. Record, CASEIB 2001*, pp. 241-243, 2001

[3] J. Rogowska, K. Jr. Preston, H.J. Aronen, G.L. Wolf. A comparative analysis of similarity mapping and eigenimaging as applied to dynamic MR imaging of low grade astrocytoma. *Acta Radiologica*, 35: 371-377, 1994

[4] J. Rogowska, K. Preston, G.J. Hunter, L.M. Hamberg, K.K. Kwong, O. Salonen, G.L. Wolf. Applications of similarity mapping in dynamic MRI. *IEEE Trans Med Imag.,* 14: 480-486, 1995

[5] G. Brix, J. Zaers, L.E. Adam, M.E. Bellemann, H. Ostertag, H. Trojan, U. Haberkorn, J. Doll, F. Oberdorfer, W.J. Lorenz. Performance evaluation of a whole-body PET scanner using the NEMA protocol. *J Nucl Med*, 38(10):1614-23, 1997

[6] L.E. Adam, J. Zaers, J., H. Ostertag, H. Trojan, M.E. Bellemann, G. Brix. Performance evaluation of the whole-body PET scanner ECAT EXACT HR/sup +/ following the IEC standard. *IEEE Trans. Nucl. Sci*., 44(3): 1172 –1179, 1997

[7] G. Kontaxakis, L. G. Strauss, T. Thireou, M. J. Ledesma-Carbayo, A. Santos, S. Pavlopoulos and A. Dimitrakopoulou-Strauss. Iterative image reconstruction for clinical PET using ordered subsets, median root prior and a Web-based interface. *Mol. Imag. Biol*., 4(3): pp. 219-231, 2002

[8] L. G. Strauss, P.S. Conti. The applications of PET in clinical oncology. *J Nucl Med*, 32: 623-648. 1991

[9] F.A. Lucas-Quesada, U. Sinha, S. Sinha. Segmentation strategies for breast tumors from dynamic MR images. *JMRI*, 6: 753-763, 1996

[10] P.A. Bandettini., A. Jesmanowicz, E.C. Wong, J.S. Hyde. Processing strategies for time-course data sets in functional MRI of the human brain, *MRM*, 30: 161-173, 1993

[11] J. Rogowska, G.L. Wolf. Temporal correlation images derived from sequential MR scans. *J Comput Assist Tomogr*, 16:784-788, 1992